Published in final edited form as:
Mol Cell Neurosci. 2011 August ; 47(4): 254–264. doi:10.1016/j.mcn.2011.04.005.

Interaction of an Intracellular Pentraxin with a BTB-Kelch Protein is Associated with Ubiquitylation, Aggregation and Neuronal Apoptosis

LeinWeih Andrew Tseng[1,3] and **John L. Bixby**[1,2,3,4,5]

[1] Dept. of Molecular and Cellular Pharmacology, University of Miami Miller School of Medicine, Miami, FL

[2] Dept. of Neurological Surgery, University of Miami Miller School of Medicine, Miami, FL

[3] Miami Project to Cure Paralysis, University of Miami Miller School of Medicine, Miami, FL

[4] Neuroscience Program, University of Miami Miller School of Medicine, Miami, FL

Abstract

Neuronal pentraxin with chromo domain (NPCD) comprises a group of neuronally expressed pentraxins with both membrane and cytosolic isoforms; the functions of cytosolic NPCD isoforms are not clear. Here, we demonstrate that a cytosolic NPCD isoform selectively interacts with the BTB-Kelch protein Mayven/Kelch-like 2 (KLHL2), an actin-binding protein implicated in process outgrowth in oligodendrocytes. The KLHL2-NPCD interaction was identified by a yeast two-hybrid screen and confirmed through colocalization and co-immunoprecipitation studies. Truncation analysis indicates that the kelch domains of KLHL2 interact with the pentraxin domain of NPCD. NPCD forms protein inclusion bodies (aggresomes) when overexpressed in tissue culture cells, KLHL2 localizes to these aggresomes, and overexpression of KLHL2 increases NPCD aggresome formation. Since other members of the BTB-Kelch family can act as Cullin-RING type E3 ubiquitin ligases, we tested the potential role of KLHL2 as a ubiquitin ligase for NPCD. We found that KLHL2 interacts selectively with cullin 3, a key component of BTB-Kelch ubiquitin ligase complexes. Further, overexpression of KLHL2 promotes NPCD ubiquitylation. Together, these results suggest a novel E3 ubiquitin ligase function of KLHL2, with NPCD as a substrate. As the formation of aggresomes is often associated with protein aggregation in neurodegenerative diseases, we tested the effects of NPCD overexpression and KLHL2 coexpression on neuronal viability. Overexpression of NPCD in hippocampal neurons led to cell death and apoptosis; this effect was exacerbated by KLHL2 co-expression. Our findings implicate KLHL2 in ubiquitin ligase activity, and suggest potential roles of NPCD and KLHL2 in neurodegeneration.

Keywords

neuronal pentraxin; neurodegeneration; aggresome; ubiquitylation; kelch-like

[5]Address correspondence to: John L. Bixby, LPLC Room 4-17, Miami Project to Cure Paralysis, 1095 NW 14th Terrace, Miami, FL 33136, 305-243-4874; FAX 305-243-3921, jbixby@miami.edu.

Introduction

Neuronal pentraxins have been implicated in synaptic refinement and plasticity, neuronal differentiation, and neurodegenerative disease (Dodds *et al.* 1997, Kirkpatrick *et al.* 2000, Xu *et al.* 2003a, Chen & Bixby 2005b, Abad *et al.* 2006, Bjartmar *et al.* 2006, Cho *et al.* 2008, Moran *et al.* 2008). Three genes encode neuronal pentraxins: neuronal pentraxin 1 (NP1), neuronal pentraxin 2 (NP2), and neuronal pentraxin with chromo domain (NPCD) (Schlimgen *et al.* 1995, Tsui *et al.* 1996, Dodds et al. 1997, Chen & Bixby 2005a). NP1 and NP2 are known as secreted proteins with a number of suggested functions in neuronal development. The best-studied product of the NPCD gene is a transmembrane protein called neuronal pentraxin receptor (NPR), but this gene also encodes several cytoplasmic isoforms in which a chromobox homolog (Cbx) domain is fused to the pentraxin domain (Chen & Bixby 2005a, Chen & Bixby 2005b). The NPR isoform of NPCD interacts with NP1 and NP2 to regulate synapse formation and synaptic plasticity (Cho et al. 2008, Kirkpatrick et al. 2000, Bjartmar et al. 2006). The function of cytosolic NPCD isoforms is less clear, though RNAi knockdown suggests a role in neuronal process outgrowth (Chen & Bixby 2005b). One approach to understanding the functions of cytosolic NPCD isoforms is to identify protein interaction partners. We therefore performed a yeast two-hybrid screen using the pentraxin domain of NPCD as the bait, and identified the BTB-Kelch family protein Mayven/Kelch-like 2 (KLHL2) as a strong binding partner.

KLHL2 is an actin-binding protein highly expressed in the brain; it has been implicated in oligodendrocyte process outgrowth as well as transcriptional regulation of growth promoting factors in breast cancer cells (Bu *et al.* 2005, Jiang *et al.* 2005, Soltysik-Espanola *et al.* 1999, Williams *et al.* 2005, Montague *et al.* 2010). KLHL2 belongs to the BTB-Kelch protein family, a group of ~50 proteins sharing an N-terminal BTB (bric a brac, tramtrack, and broad complex) or POZ (poxvirus zinc finger) domain and several C-terminal kelch repeats (Stogios *et al.* 2005).

The BTB domain is a protein-protein interaction motif (Perez-Torrado *et al.* 2006, Zollman *et al.* 1994), and the kelch repeats form a protein-interaction beta-propeller structure, initially identified as binding to and stabilizing actin filaments (Li *et al.* 2004, Xue & Cooley 1993). Several members of the BTB-Kelch protein family have been recently described as components of multi-protein complexes known as Cullin-RING E3 ubiquitin ligases (CRLs) (Furukawa *et al.* 2003, Krek 2003, Pintard *et al.* 2004, Xu *et al.* 2003b). CRLs are involved in the identification and targeting of proteins for ubiquitylation. BTB-Kelch proteins function as substrate adapters, recruiting proteins destined for ubiquitylation into the CRL complex. The large number of BTB-Kelch proteins is thought to comprise a pool of unique substrate adapters, enabling the identification of a wide range of substrates for ubiquitylation (Stogios et al. 2005).

Ubiquitylation is a post-translational modification that can regulate protein function, distribution, and stability; polyubiquitylation of proteins can lead to recognition and degradation via the 26S proteasome (Bochtler *et al.* 1999). Impairment of proteasome function can lead to the accumulation and aggregation of ubiquitylated proteins, and the formation of protein inclusion bodies, known as aggresomes, containing these proteins (Johnston *et al.* 1998). Aggresomes are detergent-insoluble perinuclear structures, containing not only the ubiquitylated and aggregated proteins, but also components of the protein ubiquitylation, degradation, and folding machinery (Kopito & Sitia 2000). Proteins described to form aggresomes when overexpressed in cultured cells are often associated with protein deposition and neurodegenerative diseases such as Alzheimer's disease (AD), Parkinson's disease (PD), Huntington's disease (HD), and prion diseases. In the case of HD, mutation of the Huntingtin protein, leading to expanded glutamine repeats, results in

increased aggregation and accumulation (Beaudoin *et al.* 2008). An aggregation-prone isoform of the neuronal protein synphilin-1 (synphilin-1A) forms aggresomes, causes neuronal death, and is present in protein deposits seen in the brains of patients with PD (Eyal *et al.* 2006).

We report that cytosolic NPCD interacts selectively with KLHL2 in mammalian cells, and that overexpressed NPCD colocalizes with KLHL2 in aggresomes. KLHL2 also interacts with cullin 3, and overexpression of KLHL2 increases ubiquitylation of NPCD and the formation of NPCD-dependent aggresomes. Finally, overexpression of NPCD in neurons leads to apoptotic death, which is exacerbated by KLHL2. Our results suggest that KLHL2 is an E3 ubiquitin ligase, and that cytosolic NPCD is among its substrates. Our results are also consistent with the idea that regulation of NPCD expression and its ubiquitylation are important in neurodegeneration.

Materials and Methods

Yeast two-hybrid screen

Yeast two-hybrid screens were performed using the Mate & Plate Mouse Embryo 17-day cDNA library in yeast strain Y187 (*MAT*α *ura3-52 his3-200 ade2-101 trp1-901 leu2-3,112 gal4Δ met–gal80Δ MEL1 URA3::GAL1*$_{UAS}$*-GAL1*$_{TATA}$*-lacZ*) from Clontech. Sequences encoding exons 1–5 or 7–10 of *Npcd* (AY395907) were fused in frame to the GAL4 DNA binding domain coding sequence in the pGBDU-C1 vector and transformed into yeast strain pJ69-4A (*MAT*a *trp1-901 leu2-3,112 ura3-52 his3-200 gal4Δ gal80Δ LYS2::GAL1-HIS3 GAL2-ADE2 met2::GAL7-lacZ*), a kind gift from Dr. Sandra Lemmon, University of Miami (James, et al., 1996). Library screening was performed by mating the pretransformed Mouse Embryo 17-day cDNA library in strain Y187 with pJ69-4A containing a NPCD bait and selection of candidate two hybrid interaction clones for expression of *LEU2*, *URA3*, *ADE2*, and *MEL1*. Candidate clones were plated on 5-FOA to lose the URA3 bait plasmid, and then retested to eliminate self-activating prey plasmids. Prey plasmids were isolated from positive clones by shuttling into bacteria and sequenced. To confirm the interaction, purified prey plasmid was co-transformed with the NPCD bait plasmid into pJ69-4A and rechecked for growth on SD-Leu-Ura-Ade medium.

Plasmid transfection

Plasmids—Full length cDNA sequences for NPCD (Isoform IV, 1.1kb variant), Mayven/KLHL2, and KEAP1 were PCR-amplified using Phusion high-fidelity polymerase (New England BioLabs), cut with restriction enzymes, and directly ligated in frame into the MCS of both pCMV-Myc and pCMV-HA plasmids (Clontech, Mountain View, CA). Full length cDNA sequences of Mayven/KLHL2 and KEAP1, used as template for PCR-amplification, were obtained from the Open Biosystems MGC full-insert expression library. Mayven/KLHL2 truncation mutants were constructed by Phusion PCR amplification from full length Mayven/KLHL2 cDNA. Plasmids encoding HA-Cullin1, -Cullin2, and -Cullin3 were generous gifts from Dr. Mark Hannink (University of Missouri) and were constructed in the pCI- HA expression vector (Clontech). Expression plasmids for fluorescently tagged NPCD domains were constructed using *Taq* PCR amplification, ligation into pGEM-T Easy, digestion with restriction enzymes, and ligation into the pEGFP-N2 expression vector (Clontech). All plasmids were sequenced to confirm sequence fidelity. Expression plasmids for mCherry/mVenus-NPCD and mCherry/mVenus- Mayven/KLHL2 were constructed through Phusion PCR amplification, digestion with restriction enzymes, and direct ligation into a modified pSport6 expression vector (Invitrogen). The pSport6 vector was modified by the insertion of fluorescent-tag sequence (mVenus, accession: DQ092360; mCherry, accession: AY678264) into the MCS, followed by the in-frame insertion of full length

NPCD (Isoform IV, 1.1kb variant) or full length Mayven/KLHL2 cDNA sequence. The Myc-Cherry expression plasmid was obtained from Dr. Murray Blackmore. The HA-ubiquitin plasmid (Lim *et al.* 2005) was purchased from Addgene (Addgene plasmid 17608).

HEK293T (HEK) cells were transfected using Lipofectamine 2000 essentially according to the manufacturer's recommendations. Briefly, cells were transfected at ~90% confluency; both plasmid DNA and Lipofectamine were diluted in opti-MEM media, incubated 5 min, then combined and incubated at RT 20 min prior to pipetting over the plated cells. Hippocampal neurons were transfected with the AMAXA Rat Neuron Nucleofector Kit (Lonza), using the program O-003. Plasmid DNA (3ug, or up to 5ul) for transfections was directly added into electroporation cuvettes. Neurons were gently resuspended in Nucleofector solution (100ul per transfection reaction or 1 million cells, transferred to electroporation cuvettes (100ul of cell suspension) with plasmid DNA, and cuvettes were shaken to mix. Immediately after electroporation, 500ul of RT culture media was added to each of the cuvettes and the neurons were removed from the cuvettes using the supplied plastic squeeze bulbs. Neurons were plated in equilibrated media.

Immunoprecipitation and immunoblotting

The anti-c-Myc immunoprecipitation kit (Sigma, St. Louis, MO) was used for all immunoprecipitation experiments. 30ul of affinity matrix was added to protein lysate prepared in CelLytic M Cell Lysis Reagent (Sigma) with 1x EDTA-free Complete protease inhibitor cocktail (Roche, Indianapolis, IN). Lysate was incubated at 4°C overnight with gentle end-over-end rotation in spin columns. Affinity matrix was washed by gravity flow with 10 volumes of chilled 1x IP buffer (Sigma) containing protease inhibitors, then 1x with chilled 0.1x IP buffer with protease inhibitors before boiling at 95ºC in 2x sample buffer for 10 minutes. Eluted proteins were resolved in 8% or 10% SDS-PAGE gels, transferred to nitrocellulose membrane, and probed with appropriate primary antibodies. IRDye700/800-conjugated secondary antibodies (Rockland, Gilbertsville, PA) were used to visualize blots using the Odyssey Imaging System (LI-COR Biosciences, Lincoln, NE). In most cases, samples were split into 2 aliquots and loaded in parallel on different gels for HA- and Myc immunoblotting.

Immunocytochemistry and imaging

For colocalization and confocal microscopy experiments, transfected HEK cells were trypsinized 24h post-transfection and allowed to adhere to glass coverslips for 12h in culture before fixation using 4% paraformaldehyde with 4% sucrose in PBS for 15 minutes at RT. Fixed cells were washed with PBS, blocked and permeabilized (2% fish gelatin and 0.03% Triton X-100 in PBS overnight at 4ºC), and stained with Hoechst nuclear stain and appropriate antibodies. Stained and washed cells were mounted onto microscope slides using Prolong Gold antifade reagent (Invitrogen, Carlsbad, CA). Images were scanned using a Zeiss LSM510 confocal microscope. For wide-field microscopy, cells were plated and visualized on tissue culture plastic using a Nikon TE200 inverted fluorescence microscope.

In-vivo ubiquitylation assay

A total of 5ug plasmid DNA was used for transfection of each well of a 6-well culture plate: 1ug of plasmid expressing HA-ubiquitin, 2ug of plasmid expressing either Myc-Cherry or Myc-NPCD, and 2ug of plasmid expressing either mVenus or mVenus-KLHL2. Cells were viewed at 24h post-transfection to confirm expression before incubation in SDS lysis buffer (2% SDS, 1% NaCl, and 0.2% Tris-HCl, pH 8) at RT with incubation at 95º C for 20 minutes followed by vortexing. Protein lysate was diluted with the same lysis buffer without

SDS to a final SDS concentration of 0.5% before use in the standard immunoprecipitation procedure. Substrate proteins were detected by Western blot as described.

Protein fractionation

A total of 4ug of plasmid DNA was used in transfection of each well of a 6-well culture plate: 2ug of HA-NPCD and 2ug of either pCMV-Myc, Myc-KLHL2 or Myc-BTB-BACK. 10h and 20h post-transfection, cells were lysed with CelLytic M Lysis Reagent (see above). Soluble protein (supernatant) was removed after centrifugation at 16,000xg to pellet the insoluble fraction. The insoluble pellet fraction was subjected to three rounds of sonication (25s, 30% Duty Cycle, 60 watt output) and ultracentrifugation (100,000 rpm, Beckman Airfuge) in CelLytic M Lysis Reagent. The resulting pellet was dissolved in sample buffer before loading.

Cell viability and TUNEL assays

The cell viability assay was performed on neuronal cultures 12h post-transfection. Calcein AM and ethidium homodimer-1 staining was performed using the Live/Dead Viability/ Cytotoxicity Kit for Mammalian Cells (Invitrogen). Cells were plated in individual 35mm plates so that staining and quantification could be done on each transfection condition individually. TUNEL staining was performed on neuronal cultures fixed at 8h post-transfection using the APO-BrdU TUNEL Assay Kit (Invitrogen). Cells were fixed using 4% paraformaldehyde with 4% sucrose on ice for 20 minutes and incubated with 70% ethanol overnight at −20º C. Staining was done according to the manufacturer's recommendations.

Antibody sources

Anti-Ubiquitin (ab19247), anti-vimentin (ab8545), and anti-Cullin3 (ab1871) antibodies were purchased from Abcam (Cambridge, MA). Anti-Hsp70 antibody (sc-65521) was purchased from Santa Cruz Biotechnology (Santa Cruz, CA). E7 monoclonal anti-β-tubulin antibody (Developmental Studies Hybridoma Bank) was used for tubulin staining in COS-7 cells. Anti-Myc-epitope (M4439), anti-HA-epitope (H9658), and anti-GAPDH (G8795) antibodies were purchased from Sigma. Alexa Fluor Dye-conjugated secondary antibodies (Invitrogen) were used in immunocytochemistry experiments: Alexa Fluor 488 (green) and Alexa Fluor 546 (red). For western blot analysis, IRDye 700/800 secondary antibodies (Rockland) were used to visualize immunoreactive bands in the Odyssey Infrared Imaging System (LI-COR Biosciences).

Quantification and Statistical Analysis

Densitometric analysis was performed using the Odyssey Infrared Imaging System. Integrated intensity was measured for discrete bands and normalized to the integrated intensity of other bands as appropriate. Monoubiquitylated Myc-NPCD as detected by anti-HA antibody (recognizing HA-ubiquitin) was normalized to total levels of Myc-NPCD as detected by anti-Myc antibody. Intensities of insoluble HA-NPCD bands were normalized to soluble NPCD within the same sample.

Aggresomes were identified based on morphology, fluorescence intensity, and size. The appearance of NPCD-containing aggresomes ranged from small punctate dots near the nucleus (~1–2uM in diameter) to large masses (~10–15uM in diameter) occupying most of the cytoplasm. NPCD-containing aggresomes were cytosolic dense masses that appeared bright compared to all other cellular fluorescence. A cell was counted as having an aggresome if it had either a small punctate aggresome or a large aggresome. HEK cell transfection efficiency was consistently at or near 100%; therefore the percentage of cells

with aggresomes was calculated by the number of cells with aggresomes divided by the total number of cells (nuclei).

Statistical significance was determined using an unpaired Student's t-test or one-way ANOVA with Tukey post-hoc test, as appropriate.

Results

The NPCD pentraxin domain interacts with kelch repeats of KLHL2

As a first step in elucidating the function of cytoplasmic NPCD isoforms, we carried out a yeast two-hybrid screen to identify interacting proteins. In a screen of 4.7 million clones using the NPCD pentraxin domain (NPCD exons 7–10) as bait, 41 of the 42 positive clones represented partial cDNAs of KLHL2 (data not shown). KLHL2 (Kelch-like 2), also known as Mayven, is an actin-binding protein highly expressed in the brain. It belongs to the BTB-Kelch family of proteins that share an N-terminal BTB domain, C-terminal kelch repeats, and usually an intervening BACK domain. Each of the interacting clones we identified encoded the BACK domain and kelch repeats of KLHL2; many were truncated and did not contain the BTB domain. These results suggest that the kelch repeats and/or the BACK domain of KLHL2 interact with the NPCD pentraxin domain.

To test the NPCD-KLHL2 interaction in mammalian cells, we performed co-immunoprecipitation experiments using full-length KLHL2 and full-length cytoplasmic NPCD. NPCD precipitated with KLHL2, but not with the related BTB-Kelch family member (and cullin-RING E3 ubiquitin ligase) Keap1/KLHL19 (Furukawa & Xiong 2005, Kobayashi *et al.* 2004), in transfected HEK cells (Fig. 1A). To investigate which region of KLHL2 mediates NPCD binding, we performed co-transfection experiments using truncation mutants of KLHL2. In these experiments all KLHL2 constructs encoding kelch domains, but no constructs lacking this domain, co-precipitated with NPCD, suggesting that the kelch repeats are necessary and sufficient for NPCD interaction (Fig. 1B).

KLHL2 and NPCD colocalize in aggresomes in transfected cells

To identify the subcellular sites of KLHL2/NPCD interaction, we examined the localization of fluorescently tagged KLHL2 and NPCD in co-transfected HEK cells. Confocal microscopy revealed that KLHL2 and NPCD most strongly colocalize in a dense, roughly spherical, perinuclear structure (Fig. 2A–C and data not shown). The location, size, and shape of these structures suggest that they are aggresomes. Aggresomes contain ubiquitylated proteins as well as components of the protein folding and degradation machinery, and are often surrounded by a cage of the intermediate filament protein vimentin (Johnston et al. 1998). As predicted, putative NPCD-containing inclusion bodies were surrounded by a vimentin cage (Fig. 2D–F), and co-localized strongly with two different aggresome markers, Hsp70 (Fig. 2G–I) and ubiquitin (Fig. 2J–L). These results indicate that exogenously expressed KLHL2 and NPCD colocalize in aggresomes. The Ptx domain of NPCD is responsible for this function, as expression of the Ptx domain, but not the Cbx domain, was sufficient for aggresomal localization (Supplementary Fig. 1).

NPCD is a substrate for KLHL2-dependent ubiquitylation

Proteins found in aggresomes are often ubiquitylated (Garcia-Mata *et al.* 1999). To test whether NPCD becomes ubiquitylated when overexpressed, we transfected HEK cells with Myc-tagged NPCD and HA-tagged ubiquitin, immunoprecipitated NPCD, and probed the precipitate with anti-HA to detect the covalent attachment of ubiquitin to NPCD. An HA-immunoreactive band, migrating at the M_r of monoubiquitylated NPCD, was present in the NPCD transfected cells and could be precipitated with anti-Myc (Fig. 3A asterisk, small

arrowhead). Additionally, a smear of HA immunoreactivity above the molecular weight of monoubiquitylated NPCD (Fig. 3A, bracketed) was precipitated by anti-Myc; this presumably corresponds to polyubiquitylated NPCD. These results indicate that NPCD can be ubiquitylated when expressed in heterologous cells.

The BTB-Kelch protein family, of which KLHL2 is a member, is a superfamily of proteins that are emerging as adapters for cullin-RING E3 ubiquitin ligases (Krek 2003, Pintard et al. 2004, Stogios & Prive 2004, Xu et al. 2003b, Furukawa et al. 2003). Though KLHL2 has not been studied in this context, the ubiquitylation of NPCD and its localization with KLHL2 in aggresomes suggest that KLHL2 may serve as an E3 ubiquitin ligase targeting NPCD. To test whether NPCD is marked for ubiquitylation by KLHL2, we performed an *in vivo* ubiquitylation assay. HEK cells were transfected with HA-ubiquitin, together with Myc-NPCD (or Myc-Cherry control) and mVenus-KLHL2 (or mVenus control). As in the previous experiment, NPCD but not mCherry became both mono- and polyubiquitylated (Fig. 3B). Interestingly, expression of KLHL2 led to an apparent increase in both mono- (arrow in Fig. 3B) and polyubiquitylated (bracket in Fig. 3B) forms of NPCD. Quantification of ubiquitylated NPCD (normalized to total precipitated NPCD) showed that KLHL2 coexpression increased NPCD monoubiquitylation by 66% (± 15%; N=3; $p < 0.05$) and polyubiquitylation by 80% (± 25%; Fig. 3B and data not shown). Our findings demonstrate that KLHL2 increases NPCD ubiquitylation and suggest that KLHL2 acts as a ubiquitin ligase for NPCD.

KLHL2 interacts with cullin 3

Ubiquitylation is a multi-step process involving three classes of enzyme: E1 ubiquitin activating enzymes, E2 ubiquitin conjugating enzymes, and E3 ubiquitin ligases (Hershko & Ciechanover 1986, Hershko & Ciechanover 1992, Pickart 2001, Scheffner *et al.* 1995). Cullin-RING E3 ubiquitin ligases are formed by the RING finger protein ROC1 (which binds to the E2 conjugating enzyme), a substrate adapter (such as the Skp1/F-box complex, or a BTB-Kelch protein), and a cullin protein that interacts with both ROC1 and the substrate adapter. All BTB-Kelch protein family members with reported E3 ubiquitin ligase activity bind to cullin 3 (Cul3) (Angers *et al.* 2006, Furukawa et al. 2003, Furukawa & Xiong 2005, Rondou *et al.* 2008). To test whether KLHL2 binds to Cul3, we expressed Myc-tagged KLHL2 and either HA-tagged Cul1, Cul2, or Cul3 in HEK cells. As expected, KLHL2 co-immunoprecipitated with Cul3, but not with Cul1 or Cul2 (Fig. 4A; asterisk). To test whether KLHL2 could interact with endogenous Cul3, we expressed Myc-KLHL2 (or a Myc-Cherry control) in HEK cells, precipitated KLHL2 with anti-Myc, and probed the precipitates with a specific Cul3 antibody. Endogenous Cul3 co-precipitated with KLHL2 (Fig. 4B; asterisk), but not with the mCherry control. Thus KLHL2 can interact with Cul3, providing further evidence for its role as a cullin-RING E3 ubiquitin ligase.

To investigate which region of KLHL2 mediates Cul3 binding, we performed co-transfection experiments using truncation mutants of KLHL2, as was previously done for NPCD binding. Strong Cul3 binding was seen with full-length KLHL2 (Fig. 4C, lane 5), and Cul3 also bound efficiently to a truncation mutant containing the BTB and BACK domains (Fig. 4C, lane 2).

Apparently weaker binding was seen with KLHL2 truncation mutants containing the BTB domain alone (Fig. 4C, lane 1) or the BACK and kelch domains (Fig. 4C, lane 3). No binding was observed with a mutant containing only the kelch domains (Fig. 4C, lane 4). These results suggest that the BTB and BACK domains of KLHL2 are required for efficient Cul3 binding, and are consistent with findings obtained with other BTB-Kelch family ubiquitin ligases.

Both HA-tagged exogenous cullins and the endogenous Cul3 protein found in HEK cells appeared as a doublet, with one band migrating at the expected M_r of ~80 kDa and a second band migrating at a M_r approximately 9 kDa higher (e.g., Fig. 4A, small arrow). The upper band is likely to represent Cul3 modified with the ubiquitin-like protein Nedd8 (Rabut & Peter 2008). Neddylation of cullins is thought to be facilitated by binding to adaptor proteins and substrates (Merlet *et al.* 2009), but we did not explore this issue in our experiments.

KLHL2 overexpression increases formation of NPCD-containing aggresomes

Polyubiquitylation of proteins can lead to proteasome-dependent degradation (Hershko & Ciechanover 1992, Thrower *et al.* 2000). For the BTB-Kelch ubiquitin ligases KLHL12 and KLHL20, coexpression with their ubiquitylation substrates led to decreased levels of these substrates (Angers et al. 2006, Lee *et al.* 2010). To test whether KLHL2 enhances proteasome-mediated degradation of NPCD, we measured levels of overexpressed NPCD in the presence and absence of co-transfected KLHL2 at 10h and 20h after transfection. We observed no differences in the level of soluble NPCD when KLHL2 was co-expressed (Fig. 5A; upper panel, open arrowhead). However, NPCD forms aggresomes when overexpressed, unlike the reported substrates of KLHL12 (Dishevelled) or KLHL20 (death-associated protein kinase [DAPK]) (Angers et al. 2006, Lee et al. 2010). As proteins found in aggresomes are detergent-insoluble, we probed the insoluble protein fraction in cells co-transfected with NPCD and KLHL2. At 10h after transfection, there was a dramatic increase in insoluble NPCD in the presence of KLHL2 compared to the control (Fig. 5A; lower panel, asterisk). At 20h after transfection, insoluble NPCD levels were more similar in KLHL2-expressing cells and controls, due to an overall increase of insoluble NPCD protein in all conditions. Quantification of insoluble NPCD levels at 10h showed a 7-fold increase with KLHL2 co-expression (Figure 5A; left graph) compared to empty plasmid (pCMV-Myc) or a mutant KLHL2 in which the kelch domains were deleted ($p < 0.01$). At 20h (Fig. 5B, right panel), values for KLHL2 co-expression were higher, but this difference did not quite reach statistical significance ($p = 0.053$).

To determine whether the increase in insoluble NPCD with KLHL2 co-expression correlated with increased aggresome formation, we expressed fluorescently-tagged NPCD in HEK cells with KLHL2, or with one of two controls: empty plasmid (pCMV-Myc) or the KLHL2 deletion mutant Myc-BTB-BACK (lacks kelch repeats). Co-expression of full-length KLHL2 led to the formation of larger NPCD-containing aggresomes at 10h after transfection (Figure 5Ba-c; arrowheads) as well as an increase in the percentage of cells with aggresomes at both 10h and 20h after transfection (Fig. 5B, graphs; $p < 0.05$). The appearance of larger aggresomes at the earlier time point is consistent with our observations of increased levels of insoluble NPCD. The increased percentage of cells containing NPCD aggresomes with KLHL2 expression could be due to the interaction of KLHL2 with NPCD. Supporting this hypothesis, the kelch domain deletion mutant of KLHL2 (Fig. 5B; BTB-BACK), which is unable to interact with NPCD, had no effect on aggresome formation compared to the controls. Since KLHL2 co-expression increases both NPCD ubiquitylation and aggresome formation, ubiquitylation of NPCD by a KLHL2-containing ligase may play a role in aggresome formation.

NPCD Expression in Neurons Causes Cytotoxicity

The accumulation of aggregated proteins in aggresomes is often studied in neurodegenerative and protein deposition disease. To explore whether NPCD overexpression can be linked to neuronal cytotoxicity, we used E18 hippocampal neurons, which endogenously express both KLHL2 and NPCD (Chen & Bixby 2005a, Chen & Bixby 2005b, Soltysik-Espanola et al. 1999). We measured cell viability in cultured hippocampal neurons in response to expression of NPCD with or without co-expression of KLHL2. Using

a live (Fig. 6A-C; green) and dead (Fig. 6D-F; red) cell double stain, we found a 40% decrease in neuronal viability in response to NPCD expression ($p<0.05$), and an 80% decrease with co-expression of KLHL2 ($p< 0.01$; Fig. 6G) compared to controls. Expression of KLHL2 alone did not increase neuronal cell death (Fig. 7 and data not shown). Since hippocampal neurons normally express cytoplasmic NPCD (Chen & Bixby 2005a), our findings suggest that appropriate regulation of NPCD expression levels is essential for neuronal viability. Presumably the aggregation and aggresome formation of NPCD seen in HEK cells is relevant to the observed neuronal cytotoxicity, as coexpression of KLHL2 exacerbates this phenotype.

KLHL2 enhances apoptotic effect of NPCD overexpression

Protein deposition diseases often lead to neuronal death via apoptotic mechanisms (Eyal et al. 2006, Morishima *et al.* 2001). To test whether overexpression of NPCD mediates neuronal cytotoxicity through apoptosis, hippocampal neurons were transfected to express KLHL2 alone, NPCD alone, KLHL2 with NPCD, or NPCD with a KLHL2 kelch domain deletion mutant (BTB-BACK). KLHL2 overexpression did not increase apoptosis, measured by TUNEL staining (Fig. 7G), over plasmid controls (Fig. 7F, K). Overexpression of NPCD increased apoptosis about 2-fold after 8h (Fig. 7H, K), which was further increased by coexpression of KLHL2 (Fig. 7I, K) compared to either empty plasmid ($p < 0.01$) or NPCD ($p < 0.05$). Thus overexpression of NPCD induces neuronal apoptosis, and coexpression of KLHL2 enhances the apoptosis-inducing effect of NPCD. The kelch domains of KLHL2 are required for enhancement of NPCD-induced apoptosis, as no increase in apoptosis was seen when the BTB-BACK mutant (lacks kelch domains) was co-expressed with NPCD (Fig. 7J, K). This observation is consistent with the idea that interaction of KLHL2 with NPCD, and increased NPCD ubiquitylation and aggregation, exacerbate apoptosis in neurons overexpressing NPCD.

Discussion

We report the identification of a novel interaction between cytosolic NPCD and the BTB-Kelch protein KLHL2. Investigation of this interaction in cultured cells showed that KLHL2 colocalizes with NPCD in aggresomes, binds both NPCD and Cul3, and increases ubiquitylation of NPCD and the rate of NPCD aggresome formation. Thus KLHL2 appears to function as a cullin-RING E3 ubiquitin ligase for NPCD. Overexpression of NPCD in primary neurons revealed a neurotoxic effect, mediated through apoptosis. Interestingly, overexpression of KLHL2 exacerbated the neuronal cytotoxicity of NPCD, suggesting the possibility that ubiquitylation and aggregation are toxic in this situation.

Exogenous overexpression of NPCD and KLHL2 resulted in strong colocalization in aggresome-like inclusion bodies, though neither protein has been found in these structures *in vivo* (Bjartmar et al. 2006, Chen & Bixby 2005a, Montague et al. 2010, Soltysik-Espanola et al. 1999). It is likely that our use of the CMV promoter leads to NPCD expression levels in excess of those normally found in neurons. Indeed, we assume that levels of cytosolic NPCD are normally tightly regulated, preventing aggresome formation. Aggresomes are normally formed when the ubiquitin proteasome degradation pathway is impaired or overwhelmed and proteins targeted for degradation accumulate and aggregate. Proteins that fold inefficiently, such as mutated forms of the cystic fibrosis transmembrane conductance regulator (CFTR), or the alternatively-spliced synphilin-1A isoform, have been reported to form aggresomes (Eyal et al. 2006, Johnston et al. 1998). Other disease associated proteins such as huntingtin, presenilin 1, alpha-synuclein, and prion protein form aggresomes when overexpressed in cultured cells (Johnston *et al.* 2002, Junn *et al.* 2002, Ma & Lindquist 2001, Taylor *et al.* 2003, Waelter *et al.* 2001). Whether cytosolic NPCD isoforms form aggresomes in neurons during stress or disease states is a topic for future studies.

NPCD-containing inclusion bodies were positive for three known aggresome markers--ubiquitin, Hsp70, and vimentin. Because of the link between ubiquitylation and aggresome formation, and because several other BTB-Kelch proteins act as components of cullin-RING E3 ubiquitin ligases (Angers et al. 2006, Furukawa & Xiong 2005, Lee et al. 2010, Rondou et al. 2008), we hypothesized that KLHL2 shares this function. All known BTB-Kelch E3 ubiquitin ligases bind selectively to Cul3 rather than other cullins (Krek 2003, Pintard et al. 2004), as we have shown for KLHL2. Further, overexpression of the BTB-Kelch E3 ubiquitin ligases KLHL12 or KLHL20 increases substrate ubiquitylation (Lee et al. 2010, Rondou et al. 2008), similar to our findings with KLHL2 and NPCD. Together with the observation that NPCD does not interact with a related BTB-Kelch protein, Keap1, our results suggest that NPCD is a specific target for ubiquitylation by a cullin-RING E3 ligase containing KLHL2.

Our truncation analysis identified the kelch domains of KLHL2 as interacting with NPCD; previous reports implicate the KLHL2 kelch repeats in actin binding (Li et al. 2004, Williams et al. 2005, Xue & Cooley 1993). Multiple binding partners have been found for kelch repeats in other cullin-RING E3 ligases. For example, the kelch repeats of Keap1 bind both to its ubiquitylation substrate Nrf2 and to actin (Ogura *et al.* 2010). Additionally, binding to two different substrates through the kelch repeats, such as dishevelled and the D4 dopamine receptor, has been reported for KLHL12 (Angers et al. 2006, Rondou et al. 2008). Because BTB-Kelch proteins appear to form homodimers (Ogura et al. 2010, Perez-Torrado et al. 2006), it is possible that KLHL2 binds actin filaments and NPCD simultaneously.

Our analysis implicates both the BTB and BACK domains of KLHL2 in Cul3 binding. BTB domains (or domains with similar structures) are considered the interaction motifs for cullin proteins (Krek 2003, Perez-Torrado et al. 2006), and these are typically associated with Cul3 interaction in other BTB-Kelch proteins (Angers et al. 2006, Furukawa & Xiong 2005). However, BTB deletion mutants of Keap1/KLHL19 and KLHL12 have also been reported to interact with Cul3 (Kobayashi et al. 2004, Rondou et al. 2008). In our experiments, a combination of the BTB and BACK domains provided the most efficient binding to Cul3, suggesting that these two domains may either cooperate or bind independently. The BACK domain has been hypothesized to function as a structural “joint,” allowing for flexibility between the BTB domain and kelch repeats (Stogios & Prive 2004). Our results suggest that the BACK domain may also play a role in Cul3 binding.

Overexpression of E3 ubiquitin ligases, and the consequent increase in substrate polyubiquitylation, is generally found to decrease levels of soluble substrate protein through ubiquitin-proteasome degradation, as is the case for KLHL12/dishevelled or KLHL20/DAPK (Angers et al. 2006, Lee et al. 2010). Overexpression of KLHL2 did not affect levels of soluble NPCD, but rather increased accumulation of detergent-insoluble NPCD and the rate of NPCD-dependent aggresome formation. Although these findings are unusual, they are not unprecedented. For example, overexpression of the E3 ubiquitin ligases, seven in absentia homolog 1 and 2 (SIAH-1, SIAH-2), promote ubiquitylation of an alternatively spliced isoform of synphilin-1 (synphilin-1A) and its accumulation in aggresomes (Eyal et al. 2006, Szargel *et al.* 2009, Liani *et al.* 2004). Synphilin-1A is an aggregation-prone ubiquitylation substrate of SIAH-1 and SIAH-2 that is found in protein deposits associated with PD, known as Lewy bodies (Liani et al. 2004). Overexpression of synphilin-1A in neurons results in apoptotic cell death, and may represent an underlying cause of neuronal degeneration through an unknown mechanism (Eyal et al. 2006). Other neurodegenerative disease-related proteins, such as alpha-synuclein and amyloid-beta, also cause apoptosis when overexpressed in neurons (van der Putten *et al.* 2000, Xu *et al.* 2002, Paradis *et al.* 1996). Similarly, we find that NPCD overexpression in hippocampal neurons promotes apoptotic cell death. Although overexpression of KLHL2 alone did not increase neuronal

apoptosis, co-expression of KLHL2 and NPCD increased apoptosis over that seen with NPCD alone. These findings indicate that the action of KLHL2 exacerbates NPCD-induced cytotoxicity. Based on our results in HEK cells, we speculate that increased NPCD ubiquitylation, driven by co-expression of KLHL2, enhances NPCD aggregation and NPCD-induced cytotoxicity in primary neurons. This idea is in line with reports that increased ubiquitylation of alpha-synuclein by its E3 ubiquitin ligases, SIAH-1 and SIAH-2, results in increased aggregation and neurotoxicity (Rott *et al.* 2008, Lee *et al.* 2008). In this system, increased synphilin-dependent aggresome formation has been linked to decreased apoptosis, suggesting a protective effect of aggresomes (Liani et al. 2004). Although KLHL2 co-expression in HEK cells is associated with an increase in NPCD-dependent aggresome formation, it is unclear whether this is also true in primary neurons, as transfected hippocampal neurons died prior to significant aggresome formation.

Our results linking dysregulation of NPCD expression to protein aggregation and neurotoxicity are interesting in light of the association between neuronal pentraxins and neurodegenerative disease. Overexpression of NP1 in cerebellar granule cells results in apoptotic neuronal cell death (DeGregorio-Rocasolano *et al.* 2001). Furthermore, NP1 expression is increased in cultured cortical neurons after exposure to the AD-associated protein amyloid-beta (Aβ); increased NP1 expression resulted in a loss of synapses, reduction in neurite outgrowth, and apoptotic neuronal death (Abad et al. 2006). NP1 levels increase in the brains of AD patients as well as in AD mouse models; in these situations, NP1 protein was found to be associated with tau protein deposits and amyloid plaques in or around dystrophic neurites (Abad et al. 2006). Similarly, NP2 is the most highly upregulated gene in the substantia nigra of patients with PD (Moran et al. 2008). Additionally, NP2 protein accumulates with alpha-synuclein in Lewy bodies, an abnormal PD-associated protein aggregate found in neuronal cytoplasm. Recently, elevated levels of 30kDa and 55 kDa species of NPCD have been associated with AD (Yin *et al.* 2009). Therefore, it is likely that dysregulation of NPCD expression, aggregation, or function may have a role in neurodegenerative disease. Further investigation of NPCD aggregation, and the regulation of its ubiquitylation state by KLHL2, may provide insight into the role of the ubiquitin machinery in protein deposition, aggregation, and cytotoxicity.

Cytosolic NPCD isoforms were first identified in a screen to identify intracellular binding partners of the receptor protein tyrosine phosphatase PTPRO, a neuronally expressed phosphatase that regulates axon growth and guidance (Chen & Bixby 2005a, Gonzalez-Brito & Bixby 2009, Shintani *et al.* 2006, Stepanek *et al.* 2005). Knockdown of NPCD in PC12 cells revealed a loss of NGF-induced process outgrowth, suggesting the possibility that NPCD and PTPRO cooperate in this function (Chen & Bixby 2005b). Similarly, KLHL2 binds actin, regulates process outgrowth in oligodendrocytes, and is expressed in both cell bodies and processes of neurons (Jiang et al. 2005, Williams et al. 2005) (Soltysik-Espanola et al. 1999). It will be interesting to explore the possibility that KLHL2 and NPCD work together to regulate axon outgrowth in neurons.

Conclusions

In summary, we have identified a novel interaction between NPCD and KLHL2, and demonstrated a novel E3 ubiquitin ligase activity of KLHL2. Additionally, we have observed that overexpression of NPCD leads to NPCD ubiquitylation, aggresome formation in HEK293T cells, and apoptosis in hippocampal neurons. Our results implicate components of the ubiquitin machinery in protein aggregation and neuronal toxicity of at least one neuronal pentraxin, and contribute to an expanding appreciation of the role of ubiquitylation and neuronal pentraxins in neurodegenerative disease.

Supplementary Material

Refer to Web version on PubMed Central for supplementary material.

Acknowledgments

We thank Dr. Mark Hannink and Dr. Murray Blackmore for their generous gifts of reagents. We thank Xuan Le for technical assistance, and Drs. Vance Lemmon, Nagi Ayad, and Hassan Al-Ali for comments on previous versions of the manuscript. This work was supported by NIH grants NS038920 and NS059866 to JLB.

Abbreviations used

AD	Alzheimer's disease
BTB	broad complex, tramtrack, and bric a brac
Cul	(cullin)
CRL	Cullin-RING E3 ubiquitin ligase
DAPK	death-associated protein kinase
HEK	HEK 293T
KLHL	kelch-like
NP	neuronal pentraxin
NPR	NP receptor
NPCD	NP with chromo domain
PD	Parkinson's disease
POZ	poxvirus zinc finger
SIAH	seven in absentia homolog

References

Abad MA, Enguita M, DeGregorio-Rocasolano N, Ferrer I, Trullas R. Neuronal pentraxin 1 contributes to the neuronal damage evoked by amyloid-beta and is overexpressed in dystrophic neurites in Alzheimer's brain. J Neurosci. 2006; 26:12735–12747. [PubMed: 17151277]

Angers S, Thorpe CJ, Biechele TL, Goldenberg SJ, Zheng N, MacCoss MJ, Moon RT. The KLHL12-Cullin-3 ubiquitin ligase negatively regulates the Wnt-beta-catenin pathway by targeting Dishevelled for degradation. Nat Cell Biol. 2006; 8:348–357. [PubMed: 16547521]

Beaudoin S, Goggin K, Bissonnette C, Grenier C, Roucou X. Aggresomes do not represent a general cellular response to protein misfolding in mammalian cells. BMC Cell Biol. 2008; 9:59. [PubMed: 18937858]

Bjartmar L, Huberman AD, Ullian EM, et al. Neuronal pentraxins mediate synaptic refinement in the developing visual system. J Neurosci. 2006; 26:6269–6281. [PubMed: 16763034]

Bochtler M, Ditzel L, Groll M, Hartmann C, Huber R. The proteasome. Annu Rev Biophys Biomol Struct. 1999; 28:295–317. [PubMed: 10410804]

Bu X, Avraham HK, Li X, Lim B, Jiang S, Fu Y, Pestell RG, Avraham S. Mayven induces c-Jun expression and cyclin D1 activation in breast cancer cells. Oncogene. 2005; 24:2398–2409. [PubMed: 15735724]

Chen B, Bixby JL. Neuronal pentraxin with chromo domain (NPCD) is a novel class of protein expressed in multiple neuronal domains. J Comp Neurol. 2005a; 481:391–402. [PubMed: 15593341]

Chen B, Bixby JL. A novel substrate of receptor tyrosine phosphatase PTPRO is required for nerve growth factor-induced process outgrowth. J Neurosci. 2005b; 25:880–888. [PubMed: 15673668]

Cho RW, Park JM, Wolff SB, et al. mGluR1/5-dependent long-term depression requires the regulated ectodomain cleavage of neuronal pentraxin NPR by TACE. Neuron. 2008; 57:858–871. [PubMed: 18367087]

DeGregorio-Rocasolano N, Gasull T, Trullas R. Overexpression of neuronal pentraxin 1 is involved in neuronal death evoked by low K(+) in cerebellar granule cells. J Biol Chem. 2001; 276:796–803. [PubMed: 11031272]

Dodds DC, Omeis IA, Cushman SJ, Helms JA, Perin MS. Neuronal pentraxin receptor, a novel putative integral membrane pentraxin that interacts with neuronal pentraxin 1 and 2 and taipoxin-associated calcium-binding protein 49. J Biol Chem. 1997; 272:21488–21494. [PubMed: 9261167]

Eyal A, Szargel R, Avraham E, Liani E, Haskin J, Rott R, Engelender S. Synphilin-1A: an aggregation-prone isoform of synphilin-1 that causes neuronal death and is present in aggregates from alpha-synucleinopathy patients. Proc Natl Acad Sci U S A. 2006; 103:5917–5922. [PubMed: 16595633]

Furukawa M, He YJ, Borchers C, Xiong Y. Targeting of protein ubiquitination by BTB-Cullin 3-Roc1 ubiquitin ligases. Nat Cell Biol. 2003; 5:1001–1007. [PubMed: 14528312]

Furukawa M, Xiong Y. BTB protein Keap1 targets antioxidant transcription factor Nrf2 for ubiquitination by the Cullin 3-Roc1 ligase. Mol Cell Biol. 2005; 25:162–171. [PubMed: 15601839]

Garcia-Mata R, Bebok Z, Sorscher EJ, Sztul ES. Characterization and dynamics of aggresome formation by a cytosolic GFP-chimera. J Cell Biol. 1999; 146:1239–1254. [PubMed: 10491388]

Gonzalez-Brito MR, Bixby JL. Protein tyrosine phosphatase receptor type O regulates development and function of the sensory nervous system. Mol Cell Neurosci. 2009; 42:458–465. [PubMed: 19800005]

Hershko A, Ciechanover A. The ubiquitin pathway for the degradation of intracellular proteins. Prog Nucleic Acid Res Mol Biol. 1986; 33:19–56. 301. [PubMed: 3025922]

Hershko A, Ciechanover A. The ubiquitin system for protein degradation. Annu Rev Biochem. 1992; 61:761–807. [PubMed: 1323239]

Jiang S, Avraham HK, Park SY, Kim TA, Bu X, Seng S, Avraham S. Process elongation of oligodendrocytes is promoted by the Kelch-related actin-binding protein Mayven. J Neurochem. 2005; 92:1191–1203. [PubMed: 15715669]

Johnston JA, Illing ME, Kopito RR. Cytoplasmic dynein/dynactin mediates the assembly of aggresomes. Cell Motil Cytoskeleton. 2002; 53:26–38. [PubMed: 12211113]

Johnston JA, Ward CL, Kopito RR. Aggresomes: a cellular response to misfolded proteins. J Cell Biol. 1998; 143:1883–1898. [PubMed: 9864362]

Junn E, Lee SS, Suhr UT, Mouradian MM. Parkin accumulation in aggresomes due to proteasome impairment. J Biol Chem. 2002; 277:47870–47877. [PubMed: 12364339]

Kirkpatrick LL, Matzuk MM, Dodds DC, Perin MS. Biochemical interactions of the neuronal pentraxins. Neuronal pentraxin (NP) receptor binds to taipoxin and taipoxin-associated calcium-binding protein 49 via NP1 and NP2. J Biol Chem. 2000; 275:17786–17792. [PubMed: 10748068]

Kobayashi A, Kang MI, Okawa H, Ohtsuji M, Zenke Y, Chiba T, Igarashi K, Yamamoto M. Oxidative stress sensor Keap1 functions as an adaptor for Cul3-based E3 ligase to regulate proteasomal degradation of Nrf2. Mol Cell Biol. 2004; 24:7130–7139. [PubMed: 15282312]

Kopito RR, Sitia R. Aggresomes and Russell bodies. Symptoms of cellular indigestion? EMBO Rep. 2000; 1:225–231. [PubMed: 11256604]

Krek W. BTB proteins as henchmen of Cul3-based ubiquitin ligases. Nat Cell Biol. 2003; 5:950–951. [PubMed: 14593416]

Lee JT, Wheeler TC, Li L, Chin LS. Ubiquitination of alpha-synuclein by Siah-1 promotes alpha-synuclein aggregation and apoptotic cell death. Hum Mol Genet. 2008; 17:906–917. [PubMed: 18065497]

Lee YR, Yuan WC, Ho HC, Chen CH, Shih HM, Chen RH. The Cullin 3 substrate adaptor KLHL20 mediates DAPK ubiquitination to control interferon responses. EMBO J. 2010

Li X, Zhang D, Hannink M, Beamer LJ. Crystal structure of the Kelch domain of human Keap1. J Biol Chem. 2004; 279:54750–54758. [PubMed: 15475350]

Liani E, Eyal A, Avraham E, et al. Ubiquitylation of synphilin-1 and alpha-synuclein by SIAH and its presence in cellular inclusions and Lewy bodies imply a role in Parkinson's disease. Proc Natl Acad Sci U S A. 2004; 101:5500–5505. [PubMed: 15064394]

Lim KL, Chew KC, Tan JM, et al. Parkin mediates nonclassical, proteasomal-independent ubiquitination of synphilin-1: implications for Lewy body formation. The Journal of neuroscience: the official journal of the Society for Neuroscience. 2005; 25:2002–2009. [PubMed: 15728840]

Ma J, Lindquist S. Wild-type PrP and a mutant associated with prion disease are subject to retrograde transport and proteasome degradation. Proc Natl Acad Sci U S A. 2001; 98:14955–14960. [PubMed: 11742063]

Merlet J, Burger J, Gomes JE, Pintard L. Regulation of cullin-RING E3 ubiquitin-ligases by neddylation and dimerization. Cell Mol Life Sci. 2009; 66:1924–1938. [PubMed: 19194658]

Montague P, Kennedy PG, Barnett SC. Subcellular localization of Mayven following expression of wild type and mutant EGFP tagged cDNAs. BMC Neurosci. 2010; 11:63. [PubMed: 20504342]

Moran LB, Hickey L, Michael GJ, Derkacs M, Christian LM, Kalaitzakis ME, Pearce RK, Graeber MB. Neuronal pentraxin II is highly upregulated in Parkinson's disease and a novel component of Lewy bodies. Acta Neuropathol. 2008; 115:471–478. [PubMed: 17987278]

Morishima Y, Gotoh Y, Zieg J, Barrett T, Takano H, Flavell R, Davis RJ, Shirasaki Y, Greenberg ME. Beta-amyloid induces neuronal apoptosis via a mechanism that involves the c-Jun N-terminal kinase pathway and the induction of Fas ligand. J Neurosci. 2001; 21:7551–7560. [PubMed: 11567045]

Ogura T, Tong KI, Mio K, Maruyama Y, Kurokawa H, Sato C, Yamamoto M. Keap1 is a forked-stem dimer structure with two large spheres enclosing the intervening, double glycine repeat, and C-terminal domains. Proc Natl Acad Sci U S A. 2010; 107:2842–2847. [PubMed: 20133743]

Paradis E, Douillard H, Koutroumanis M, Goodyer C, LeBlanc A. Amyloid beta peptide of Alzheimer's disease downregulates Bcl-2 and upregulates bax expression in human neurons. J Neurosci. 1996; 16:7533–7539. [PubMed: 8922409]

Perez-Torrado R, Yamada D, Defossez PA. Born to bind: the BTB protein-protein interaction domain. Bioessays. 2006; 28:1194–1202. [PubMed: 17120193]

Pickart CM. Mechanisms underlying ubiquitination. Annu Rev Biochem. 2001; 70:503–533. [PubMed: 11395416]

Pintard L, Willems A, Peter M. Cullin-based ubiquitin ligases: Cul3-BTB complexes join the family. EMBO J. 2004; 23:1681–1687. [PubMed: 15071497]

Rabut G, Peter M. Function and regulation of protein neddylation. 'Protein modifications: beyond the usual suspects' review series. EMBO Rep. 2008; 9:969–976. [PubMed: 18802447]

Rondou P, Haegeman G, Vanhoenacker P, Van Craenenbroeck K. BTB Protein KLHL12 targets the dopamine D4 receptor for ubiquitination by a Cul3-based E3 ligase. J Biol Chem. 2008; 283:11083–11096. [PubMed: 18303015]

Rott R, Szargel R, Haskin J, Shani V, Shainskaya A, Manov I, Liani E, Avraham E, Engelender S. Monoubiquitylation of alpha-synuclein by seven in absentia homolog (SIAH) promotes its aggregation in dopaminergic cells. J Biol Chem. 2008; 283:3316–3328. [PubMed: 18070888]

Scheffner M, Nuber U, Huibregtse JM. Protein ubiquitination involving an E1-E2-E3 enzyme ubiquitin thioester cascade. Nature. 1995; 373:81–83. [PubMed: 7800044]

Schlimgen AK, Helms JA, Vogel H, Perin MS. Neuronal pentraxin, a secreted protein with homology to acute phase proteins of the immune system. Neuron. 1995; 14:519–526. [PubMed: 7695898]

Shintani T, Ihara M, Sakuta H, Takahashi H, Watakabe I, Noda M. Eph receptors are negatively controlled by protein tyrosine phosphatase receptor type O. Nat Neurosci. 2006; 9:761–769. [PubMed: 16680165]

Soltysik-Espanola M, Rogers RA, Jiang S, Kim TA, Gaedigk R, White RA, Avraham H, Avraham S. Characterization of Mayven, a novel actin-binding protein predominantly expressed in brain. Mol Biol Cell. 1999; 10:2361–2375. [PubMed: 10397770]

Stepanek L, Stoker AW, Stoeckli E, Bixby JL. Receptor tyrosine phosphatases guide vertebrate motor axons during development. J Neurosci. 2005; 25:3813–3823. [PubMed: 15829633]

Stogios PJ, Downs GS, Jauhal JJ, Nandra SK, Prive GG. Sequence and structural analysis of BTB domain proteins. Genome Biol. 2005; 6:R82. [PubMed: 16207353]

Stogios PJ, Prive GG. The BACK domain in BTB-kelch proteins. Trends Biochem Sci. 2004; 29:634–637. [PubMed: 15544948]

Szargel R, Rott R, Eyal A, Haskin J, Shani V, Balan L, Wolosker H, Engelender S. Synphilin-1A inhibits seven in absentia homolog (SIAH) and modulates alpha-synuclein monoubiquitylation and inclusion formation. J Biol Chem. 2009; 284:11706–11716. [PubMed: 19224863]

Taylor JP, Tanaka F, Robitschek J, Sandoval CM, Taye A, Markovic-Plese S, Fischbeck KH. Aggresomes protect cells by enhancing the degradation of toxic polyglutamine-containing protein. Hum Mol Genet. 2003; 12:749–757. [PubMed: 12651870]

Thrower JS, Hoffman L, Rechsteiner M, Pickart CM. Recognition of the polyubiquitin proteolytic signal. EMBO J. 2000; 19:94–102. [PubMed: 10619848]

Tsui CC, Copeland NG, Gilbert DJ, Jenkins NA, Barnes C, Worley PF. Narp, a novel member of the pentraxin family, promotes neurite outgrowth and is dynamically regulated by neuronal activity. J Neurosci. 1996; 16:2463–2478. [PubMed: 8786423]

van der Putten H, Wiederhold KH, Probst A, et al. Neuropathology in mice expressing human alpha-synuclein. J Neurosci. 2000; 20:6021–6029. [PubMed: 10934251]

Waelter S, Boeddrich A, Lurz R, Scherzinger E, Lueder G, Lehrach H, Wanker EE. Accumulation of mutant huntingtin fragments in aggresome-like inclusion bodies as a result of insufficient protein degradation. Mol Biol Cell. 2001; 12:1393–1407. [PubMed: 11359930]

Williams SK, Spence HJ, Rodgers RR, Ozanne BW, Fitzgerald U, Barnett SC. Role of Mayven, a kelch-related protein in oligodendrocyte process formation. J Neurosci Res. 2005; 81:622–631. [PubMed: 16035103]

Xu D, Hopf C, Reddy R, et al. Narp and NP1 form heterocomplexes that function in developmental and activity-dependent synaptic plasticity. Neuron. 2003a; 39:513–528. [PubMed: 12895424]

Xu J, Kao SY, Lee FJ, Song W, Jin LW, Yankner BA. Dopamine-dependent neurotoxicity of alpha-synuclein: a mechanism for selective neurodegeneration in Parkinson disease. Nat Med. 2002; 8:600–606. [PubMed: 12042811]

Xu L, Wei Y, Reboul J, Vaglio P, Shin TH, Vidal M, Elledge SJ, Harper JW. BTB proteins are substrate-specific adaptors in an SCF-like modular ubiquitin ligase containing CUL-3. Nature. 2003b; 425:316–321. [PubMed: 13679922]

Xue F, Cooley L. kelch encodes a component of intercellular bridges in Drosophila egg chambers. Cell. 1993; 72:681–693. [PubMed: 8453663]

Yin GN, Lee HW, Cho JY, Suk K. Neuronal pentraxin receptor in cerebrospinal fluid as a potential biomarker for neurodegenerative diseases. Brain research. 2009; 1265:158–170. [PubMed: 19368810]

Zollman S, Godt D, Prive GG, Couderc JL, Laski FA. The BTB domain, found primarily in zinc finger proteins, defines an evolutionarily conserved family that includes several developmentally regulated genes in Drosophila. Proc Natl Acad Sci U S A. 1994; 91:10717–10721. [PubMed: 7938017]

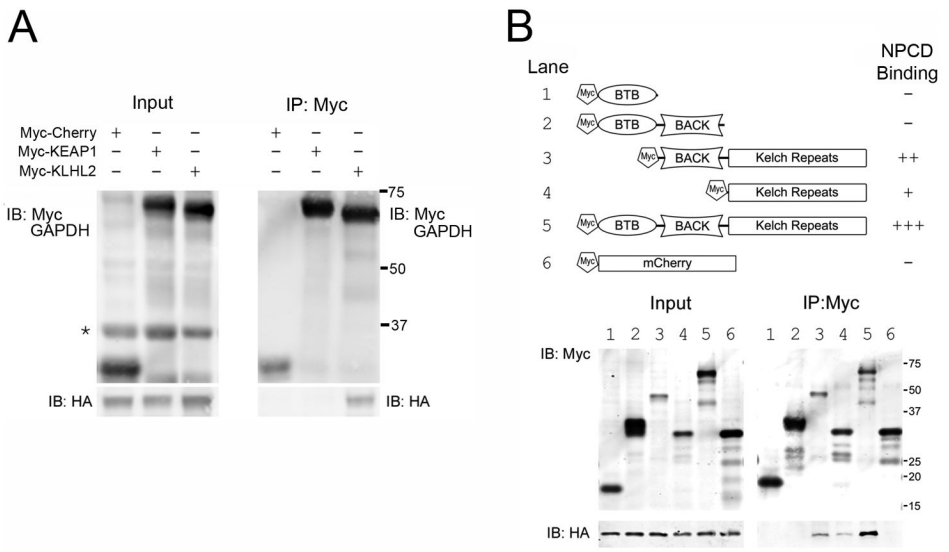

Figure 1.

Selective co-immunoprecipitation of NPCD with KLHL2 containing Kelch domains. **A.** HEK cells were transfected with HA-NPCD and either Myc-Cherry, Myc-Keap1, or Myc-KLHL2. 48h post-transfection, protein lysate (Input) or anti-Myc immunoprecipitate (IP: Myc) was subjected to SDS-PAGE and Western blot with anti-Myc, anti-HA, and anti-GAPDH (control, asterisk). All 4 constructs were expressed (Input), and each of the 3 Myc constructs (but not GAPDH) were immunoprecipitated. HA-NPCD co-immunoprecipitated with Myc-KLHL2 but not with Myc-Cherry or Myc-Keap1 (IB: HA). **B.** HEK cells were transfected with HA-NPCD and one of the Myc expression constructs illustrated at top: (1) Myc-BTB, (2) Myc-BTB-BACK, (3) Myc-BACK-Kelch, (4) Myc-Kelch, (5) Myc-KLHL2, or (6) Myc-Cherry. Protein lysate and anti-Myc immunoprecipitate were subjected to SDS-PAGE and Western blot as in **A**. All constructs were expressed, but HA-NPCD co-immunoprecipitated only with Myc-BACK-Kelch, Myc-Kelch, and Myc-KLHL2 (lanes 3, 4, and 5). Similar results were seen in a second experiment.

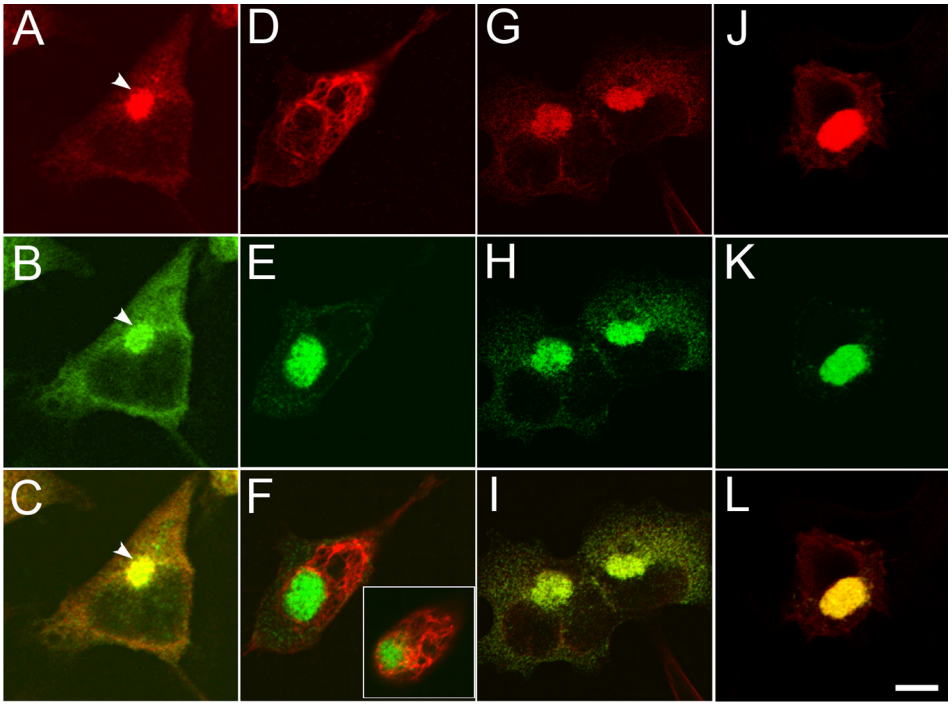

Figure 2.

NPCD colocalizes with KLHL2 and aggresome markers. **A–C**. HEK cells were transfected with mCherry-KLHL2 (**A**, red) and mVenus-NPCD (**B**, green). After 48h, confocal microscopy shows strong colocalization in large perinuclear structures (arrowheads; overlay in **C**). **D–L**. HEK cells were transfected with mVenus-NPCD (green; **E, H, K**). After 48h, cells were fixed and stained with antibodies against vimentin (**D**, red), Hsp70 (**G**, red), or ubiquitin (**J**, red); overlays are shown in **F**, **I**, and **L**. (**D–F**) Confocal microscopy of an optical slice through the NPCD-containing structure showed an encircling vimentin ring (**F**). A second optical slice (inset, **F**) shows the cage-like appearance of vimentin forming around the NPCD structure. (**G-I**) Hsp70 immunostaining (red) colocalized with NPCD expression (green) in large perinuclear aggregates and to some degree in cytosolic puncta. (**J–L**) Ubiquitin immunostaining (red) showed strong colocalization with NPCD (green). Scale bar, 10uM.

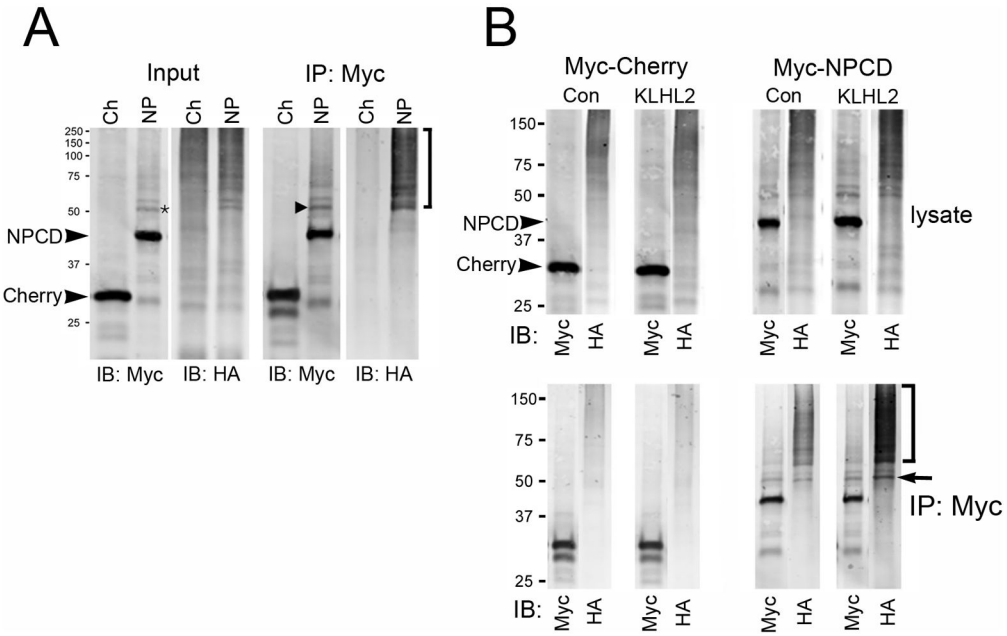

Figure 3.

NPCD is a ubiquitin ligase substrate. **A**. HEK cells were transfected with HA-Ubiquitin and either Myc-Cherry or Myc-NPCD. After 24h, cell lysate (Input) or Myc immunoprecipitate (IP: Myc) was subjected to SDS-PAGE and probed with anti-Myc or anti-HA. Myc-Cherry and Myc-NPCD were precipitated in similar amounts (labeled arrowheads). A Myc-immunoreactive band migrating 9 kDa above Myc-NPCD, corresponding to monoubiquitylated NPCD, was immunoprecipitated by anti-Myc (asterisk, small arrowhead). An HA-immunoreactive smear, corresponding to total ubiquitylated proteins, was seen in both Myc-Cherry and Myc-NPCD expressing cells; ubiquitylated proteins above the MW of Myc-NPCD (brackets) were enriched in Myc-NPCD expressing cells and immunoprecipitated by anti-Myc. **B**. In-Vivo Ubiquitylation by KLHL2. HEK cells were transfected with HA-Ubiquitin, one of two substrates (Myc-Cherry or Myc-NPCD), and mVenus-KLHL2 or mVenus (Con). Total lysates (upper blots), and anti-Myc immunoprecipitates (lower blots) were subjected to Western blotting with anti-Myc and anti-HA. (Upper Left) Cells expressing Myc-Cherry showed no difference in total ubiquitylation (IB: HA) in response to mVenus-KLHL2. (Lower Left) Immunoprecipitation of Myc-Cherry did not co-precipitate ubiquitylated proteins. (Upper Right) Cells expressing Myc-NPCD showed increased ubiquitylation at M_rs above that of NPCD when mVenus-KLHL2 was expressed. (Lower Right) Immunoprecipitation of Myc-NPCD co-precipitated ubiquitylated proteins the size of monoubiquitylated NPCD (arrow) and above (bracket); levels of these ubiquitylated NPCD species were higher with KLHL2 expression. Similar results were seen in a second experiment.

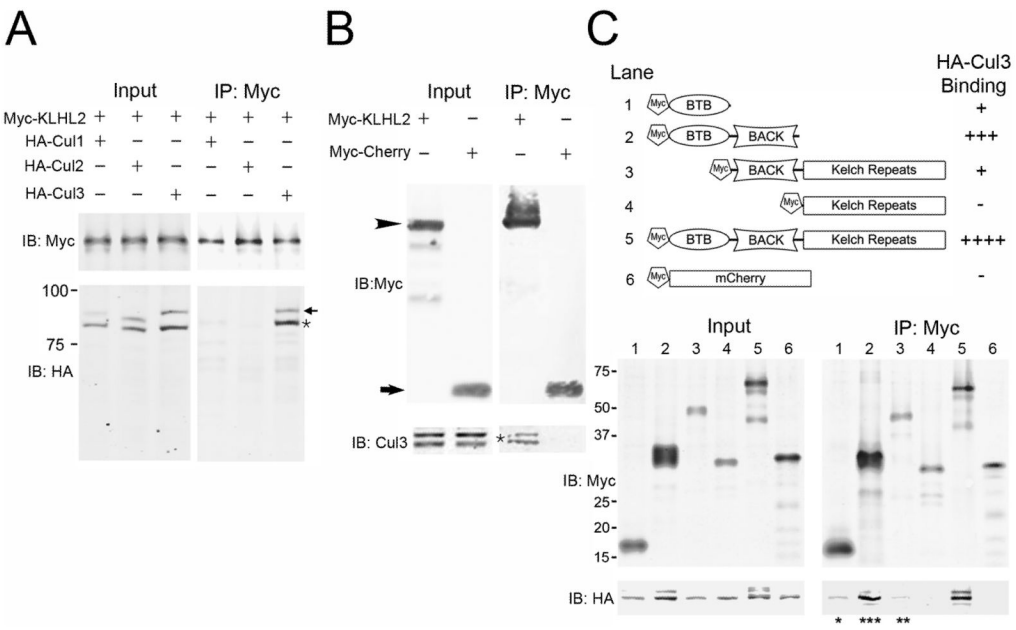

Figure 4.

KLHL2 interacts with Cul3 through the BTB-BACK domain. **A.** HEK cells were transfected with Myc-KLHL2 and either HA-Cul1, HA-Cul2, or HA-Cul3. After 48h, lysates (Input) and Myc immunoprecipitates (IP: Myc) were blotted with anti-Myc and anti-HA. Although all three cullin isoforms were expressed, only HA-Cul3 co-immunoprecipitated with Myc-KLHL2 (asterisk). The bands 9kDa above each cullin (arrow) are likely to be neddylated forms of the respective cullin proteins. **B.** HEK cells were transfected with either Myc-KLHL2 or Myc-Cherry control, and subjected to immunoprecipitation and Western blotting as in A. Endogenous Cul3 protein co-precipitated with Myc-KLHL2 (asterisk), but not Myc-Cherry. **C.** HEK cells were transfected with HA-Cul3 and one of the following: (1) Myc-BTB, (2) Myc-BTB-BACK, (3) Myc-BACK-Kelch, (4) Myc-Kelch, (5) Myc-KLHL2, or (6) Myc-Cherry and subjected to immunoprecipitation and Western blotting after 48h. A variable level of both neddylation and expression was seen with HA-Cul3 (Input, IB: HA). All Myc-tagged constructs were immunoprecipitated. HA-Cul3 co-immunoprecipitated with Myc-BTB (lane 1; asterisk), Myc-BACK-Kelch (lane 3; double asterisk), Myc-BTB-BACK (lane 2; triple asterisk) and Myc-KLHL2 (lane 5); association with the BTB-BACK mutant and full-length KLHL2 appeared quantitatively the strongest. Similar results were seen in a second experiment.

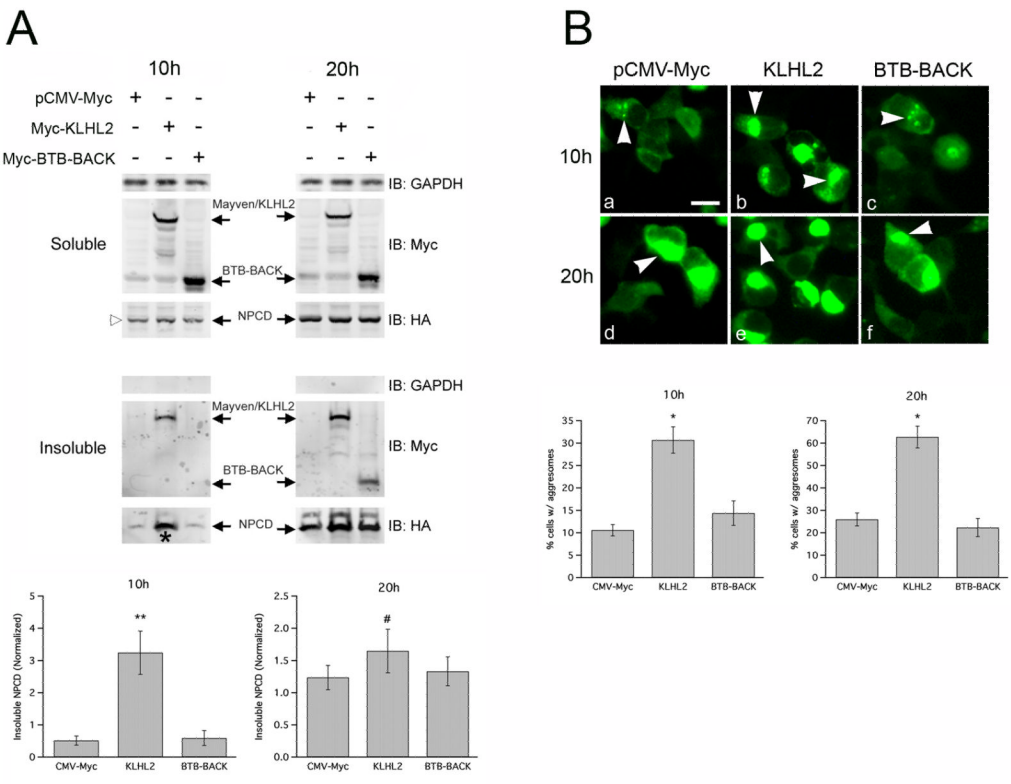

Figure 5.

KLHL2 expression increases both distribution of NPCD into the insoluble fraction and aggresome formation. **A.** HEK cells were transfected with HA-NPCD and either pCMV-Myc, Myc-KLHL2, or Myc-BTB-BACK. 10h and 20h post-transfection, cells were harvested and separated into soluble and insoluble fractions before SDS-PAGE and Western blotting. GAPDH was present in the soluble fraction (upper blots) but not the insoluble fraction (lower blots). At 10h, all expressed proteins were present in the soluble fraction, and substantial Myc-KLHL2 but not Myc-BTB-BACK was present in the insoluble fraction. Insoluble NPCD was strongly increased by expression of Myc-KLHL2. At 20h, both Myc-KLHL2 and Myc-BTB-BACK were present in the insoluble fraction. Graphs: At 10h post-transfection, the relative amount of insoluble NPCD was significantly increased by KLHL2 expression (N= 3, one-way ANOVA with Tukey post-hoc tests; ** = $p < 0.01$). No difference was seen between control and Myc-BTB-BACK coexpression conditions. At 20h post-transfection, insoluble HA-NPCD appeared to be increased by Myc-KLHL2, but this increase did not reach statistical significance (N=3, one-way ANOVA with Tukey post-hoc tests; #; $p = 0.053$). **B.** HEK cells were transfected with mVenus-NPCD (green) and either pCMV-Myc (**a, d**), Myc-KLHL2 (**b, e**), or Myc-BTB-BACK (**c, f**). Cells were fixed 10h or 20h post-transfection. (**a-c**) 10h post-transfection, cells transfected with control plasmids or Myc-BTB-BACK showed small punctate structures in a small percentage of cells (arrowheads). Cells transfected with Myc-KLHL2 showed the formation of larger aggresomes in a higher number of cells. (**d-f**) 20h post-transfection, larger aggresomes (arrowheads) were seen in all conditions. Graphs: The percentage of cells with NPCD aggresomes increased with KLHL2 co-expression at both 10h and 20h. (N=3, one-way ANOVA with Tukey post-hoc tests; *; $p < 0.05$). No differences were seen between control plasmid and Myc-BTB-BACK transfection conditions. Scale bar = 10uM

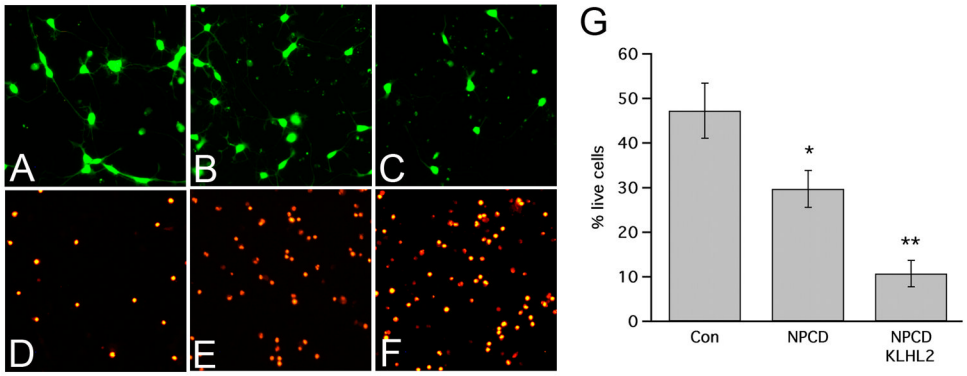

Figure 6.

NPCD overexpression and KLHL2 co-expression increase neuronal death. E18 hippocampal neurons were transfected with control plasmids (**A, D**), Myc-NPCD and pCMV-HA (**B, E**), or Myc-NPCD and HA-KLHL2 (**C, F**). 12h post-transfection, cells were stained with calcein AM (green, stains live cells) and propidium iodide (red, stains dead cells). (**A, D**) Neurons transfected with control plasmids (pCMV-Myc, pCMV-HA) looked generally healthy and showed approximately equal numbers of live and dead cells per field. (**B, E**) Neuronal cultures transfected with Myc-NPCD and pCMV-HA showed an increased percentage of dead cells. (**C, F**) In neuronal cultures transfected with Myc-NPCD and HA-KLHL2 the vast majority of cells were dead at 12h. (**G**) Cultures transfected with control plasmids showed approximately 47% cell viability (Con). Cultures transfection with Myc-NPCD and pCMV-HA (NPCD) showed a significant decrease in cell viability (to 30%). Cultures transfected with Myc-NPCD and HA-KLHL2 (NPCD/KLHL2) showed cell viability of only 11% (N=3; one-way ANOVA with Tukey post-hoc tests; * = $p < 0.05$ compared to control; ** = $p < 0.01$ compared to control, $p < 0.05$ compared to NPCD)

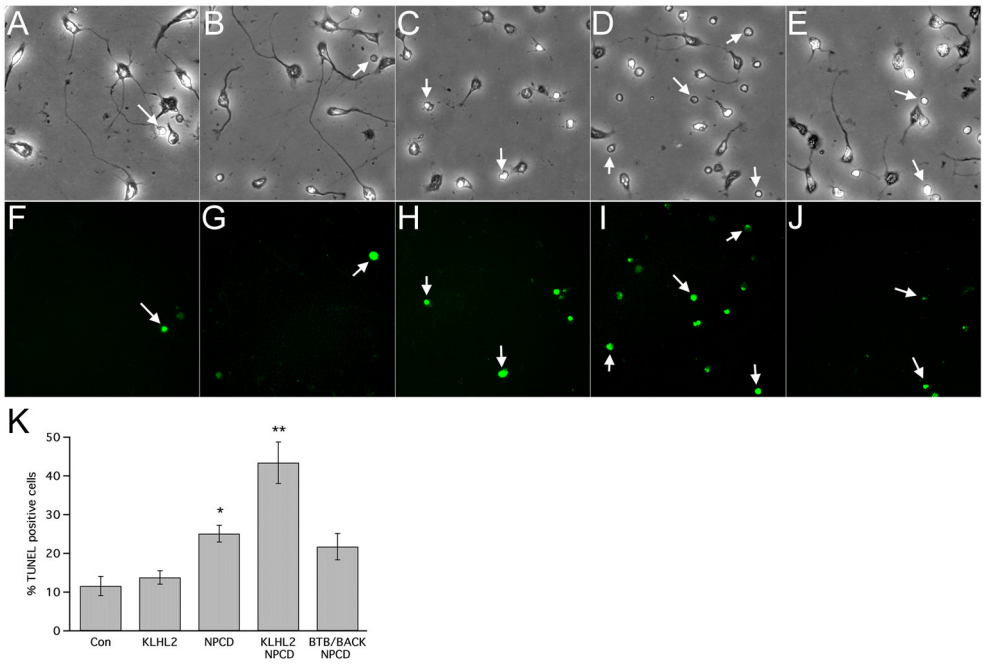

Figure 7.

NPCD overexpression and KLHL2 co-expression increase neuronal apoptosis. E18 hippocampal neurons were transfected with control plasmids (**A, F**), Myc-KLHL2 and pCMV-HA (**B, G**), HA-NPCD and pCMV-Myc (**C, H**), Myc-KLHL2 and HA-NPCD (**D, I**), or Myc-BTB-BACK and HA-NPCD (E, J). Cells were fixed and TUNEL stained (green) after 8h. (**A, F**) Neuronal cultures transfected with control plasmids looked healthy with low levels of TUNEL stained cells (arrow). (**B, G**) Expression of Myc-KLHL2 did not appear to alter cell health. (**C, H**) NPCD expression increased the number of TUNEL positive, phase-bright cells (arrows). (**D, I**) Co-expression of KLHL2 and NPCD greatly increased the number of TUNEL positive cells (arrows). (**E, J**) Co-expression of BTB-BACK and NPCD did not increase TUNEL staining above that of NPCD alone. (**K**) NPCD expression significantly increased the percentage of TUNEL positive cells, and this percentage was further increased by co-expression of KLHL2 but not the BTB-BACK mutant. (N=3, one-way ANOVA with Tukey post-hoc tests; * = $p < 0.05$ compared to control; ** = $p < 0.01$ compared to control, $p < 0.05$ when compared to NPCD)